HAL open science

Orchestrating front and rear sensors for global stabilization of unicycles

Riccardo Ballaben, Philipp Braun, Luca Zaccarian

▶ To cite this version:

Riccardo Ballaben, Philipp Braun, Luca Zaccarian. Orchestrating front and rear sensors for global stabilization of unicycles. 2022. hal-03586547

HAL Id: hal-03586547

https://hal.science/hal-03586547v1

Preprint submitted on 24 Feb 2022

HAL is a multi-disciplinary open access archive for the deposit and dissemination of scientific research documents, whether they are published or not. The documents may come from teaching and research institutions in France or abroad, or from public or private research centers.

L'archive ouverte pluridisciplinaire **HAL**, est destinée au dépôt et à la diffusion de documents scientifiques de niveau recherche, publiés ou non, émanant des établissements d'enseignement et de recherche français ou étrangers, des laboratoires publics ou privés.

Orchestrating front and rear sensors for global stabilization of unicycles

Riccardo Ballaben * **Philipp Braun** ** **Luca Zaccarian** ***

* *University of Trento (e-mail: riccardo.ballaben@studenti.unitn.it)*
** *Australian National University (e-mail: philipp.braun@anu.edu.au)*
*** *LAAS-CNRS Université de Toulouse, CNRS, Toulouse, France and University of Trento, Italy (e-mail: luca.zaccarian@laas.fr)*

Abstract: We consider mobile robots described through unicycle dynamics equipped with range sensors and cameras, one in the front and one in the back providing measurements of the distance and misalignment to a target. We derive locally asymptotically stabilizing control laws driving the robot to the target position and orientation. The local control laws are combined into a hybrid global stabilizer, switching between control laws relying on the measurements from the front and rear sensors. Using Lyapunov arguments in the local setting as well as in the hybrid systems formulation, we prove global asymptotic stability of the target set for the hybrid closed-loop system. The results are illustrated on numerical examples.

1. INTRODUCTION & MOTIVATION

Driving a robot described through unicycle dynamics to a target set with a particular fixed final orientation is a difficult task due to nonholonomic constraints. In particular, the origin of the unicycle dynamics cannot be globally asymptotically stabilized through a static state feedback Brockett (1983). Indeed unicycle dynamics do not satisfy the so-called Brockett conditions. Control laws guaranteeing convergence to the origin, thus imply the necessity to combine the controller designs with reference tracking or path following approaches or to rely on discontinuous feedback laws instead. We refer to Tzafestas (2013) as a general reference for mobile robots and control.

In this work, we follow the second path, i.e., we consider discontinuous feedback laws. While Lipschitz-continuous feedback laws guarantee some intrinsic robustness properties with respect to stability and with respect to existence and uniqueness of solutions, well-posedness and robustness is more difficult to achieve with discontinuous feedback laws (Sontag (1999)). To define a globally asymptotically stabilizing feedback we use a hybrid systems formalism and borrow results from hybrid Lyapunov theory (Goebel et al. (2012)). We define locally stabilizing control laws and orchestrate them through a switching mechanism to obtain global results. The local controller design is motivated through the results and derivations in Aicardi et al. (1995), whereas the global design and the setup are motivated and derived differently.

We consider mobile robots, which in Cartesian coordinates are described through the dynamics

$$\dot{x} = \begin{bmatrix} \dot{p}_1 \\ \dot{p}_2 \\ \dot{\phi} \end{bmatrix} = f(x,u) = \begin{bmatrix} u_1 \cos(\phi) \\ u_1 \sin(\phi) \\ u_2 \end{bmatrix}, \tag{1}$$

where $p = [p_1 \; p_2]^T \in \mathbb{R}^2$ captures the unicycle position in the plane, $\phi \in \mathbb{R}$ captures its orientation and the input $u = [u_1 \; u_2]^T \in \mathbb{R}^2$ captures the velocity and angular velocity.

⋆ P. Braun and L. Zaccarian are supported in part by the Agence Nationale de la Recherche (ANR) via grant "Hybrid And Networked Dynamical sYstems" (HANDY), number ANR-18-CE40-0010.

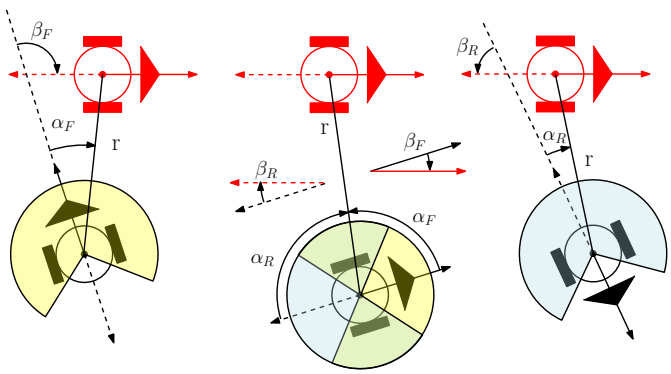

Fig. 1. The robot is equipped with range sensors and cameras (a front and a rear camera) with overlapping fields of view, providing measurements $(r, \alpha_\mathrm{F}, \beta_\mathrm{F})$ and $(r, \alpha_\mathrm{R}, \beta_\mathrm{R})$, respectively. Each measurement is only available when the target is in the camera's field of view $\alpha_i \in [-\frac{\pi}{2} - \delta, \frac{\pi}{2} + \delta]$, $i \in \{\mathrm{F}, \mathrm{R}\}$.

We assume that the mobile robot is equipped with various sensors, including a range sensor, measuring the distance $r \in \mathbb{R}_{\geq 0}$ to the target position, and two cameras (a front and a rear camera). The cameras provide measurements of the misalignment of the heading of the robot in terms of angles α_F and α_R corresponding to measurements from the front and the rear camera. In addition, the cameras provide measurements of the angles β_F and β_R, as represented in Figure 1. By combining α_i and β_i, $i \in \{\mathrm{F}, \mathrm{R}\}$, the mismatch of the robot orientation and the target orientation is defined. The setting is visualized in Figure 1, where it is apparent that, the field of view of both front and rear cameras are as follows

$$\alpha_\mathrm{F}, \alpha_\mathrm{R} \in [-\tfrac{\pi}{2} - \delta, \tfrac{\pi}{2} + \delta], \tag{2}$$

where $\delta \in (0, \frac{\pi}{2})$ induces some overlap and ensures that the combined fields of view are covering an area of 360°. While in certain configurations only one camera is available (left and right cases in Figure 1), in some configurations the target is in the field of view of both cameras. This motivates the use of a hybrid controller, which switches between measurements from the two cameras and makes

use of different error dynamics describing the mismatch of the robot and the target position and orientation.

2. ROBOT DYNAMICS

In this section we derive dynamics in local coordinates defined as $z_i = [r_i \ \beta_i \ \alpha_i]^T$, $i \in \{\mathrm{R}, \mathrm{F}\}$. The relation between the mobile robot in Cartesian coordinates and the local coordinates related to the sensor measurements, is described through the coordinate transformations

$$\begin{bmatrix} p_1 \\ p_2 \\ \phi \end{bmatrix} = \begin{bmatrix} r\cos(\alpha_\mathrm{R} - \beta_\mathrm{R}) \\ r\sin(\alpha_\mathrm{R} - \beta_\mathrm{R}) \\ -\beta_\mathrm{R} \end{bmatrix}, \quad \begin{bmatrix} p_1 \\ p_2 \\ \phi \end{bmatrix} = \begin{bmatrix} r\cos(\alpha_\mathrm{F} - \beta_\mathrm{F} - \pi) \\ r\sin(\alpha_\mathrm{F} - \beta_\mathrm{F} - \pi) \\ -\beta_\mathrm{F} \end{bmatrix} \tag{3}$$

where F and R again correspond to the front and rear cameras. The coordinate transformations (3) follow from trigonometric arguments applied to the variables defined and illustrated through Figure 2.

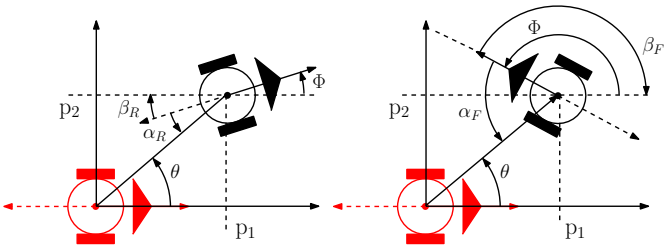

Fig. 2. Coordinate transformation from global Cartesian coordinates to local coordinates depending on the robot orientation.

The local coordinates are defined on the domain

$$z_i \in \mathcal{Z} := \mathbb{R}_{\geq 0} \times \mathbb{R} \times [-\tfrac{\pi}{2} - \delta, \tfrac{\pi}{2} + \delta], \quad i \in \{\mathrm{F}, \mathrm{R}\}, \tag{4}$$

for $\delta \in (0, \frac{\pi}{2})$, where the third component of z_i evolves in a bounded set as defined in (2). Whenever the target is in the field of view of both cameras (see the middle sketch in Figure 1), by simple geometric considerations we obtain

$$\begin{aligned} \alpha_\mathrm{F} &= \alpha_\mathrm{R} - \pi\,\mathrm{sign}(\alpha_\mathrm{R}), & \beta_\mathrm{F} &= \beta_\mathrm{R}, \\ \alpha_\mathrm{R} &= \alpha_\mathrm{F} - \pi\,\mathrm{sign}(\alpha_\mathrm{F}), & \beta_\mathrm{R} &= \beta_\mathrm{F}. \end{aligned} \tag{5}$$

Moreover, again due to the fact that $\delta > 0$ by assumption, for $r \neq 0$, i.e., $|p| \neq 0$, we can equivalently represent the robot through Cartesian coordinates x or through at least one of the local coordinates z_i, $i \in \{\mathrm{F}, \mathrm{R}\}$.

As a next step, we derive from (1) and (3) the dynamics in the local coordinates

$$\dot{z}_\mathrm{R} = f_\mathrm{R}(z_\mathrm{R}, v) \qquad \text{and} \qquad \dot{z}_\mathrm{F} = f_\mathrm{F}(z_\mathrm{F}, v), \tag{6}$$

with a transformed input $v \in \mathbb{R}^2$.

Lemma 1. Whenever $r \neq 0$, the dynamics (1) can be equivalently represented through (6) where

$$f_\mathrm{R}(z_\mathrm{R}, v) = \begin{bmatrix} v_1 r\cos(\alpha_\mathrm{R}) \\ -v_2 \\ -v_1\sin(\alpha_\mathrm{R}) - v_2 \end{bmatrix}, f_\mathrm{F}(z_\mathrm{F}, v) = \begin{bmatrix} -v_1 r\cos(\alpha_\mathrm{F}) \\ -v_2 \\ v_1\sin(\alpha_\mathrm{F}) - v_2 \end{bmatrix} \tag{7}$$

with transformed input $v_1 r = u_1$ and $v_2 = u_2$. ⌟

Proof. We start with a derivation of f_R. Let $r \neq 0$ for the remainder of the proof and define the angle $\theta = \alpha_\mathrm{R} - \beta_\mathrm{R}$.

Proceeding as in (Nešić et al., 2011, eq. (41)), we provide an alternative expression of the Jacobian $\frac{\partial p}{\partial p} = I$. In particular, using the definition of θ as well as (3), the matrix can be rewritten as

$$\begin{aligned} \frac{\partial p}{\partial p} &= \begin{bmatrix} \frac{\partial r}{\partial p_1}\cos(\theta) & \frac{\partial r}{\partial p_2}\cos(\theta) \\ \frac{\partial r}{\partial p_1}\sin(\theta) & \frac{\partial r}{\partial p_2}\sin(\theta) \end{bmatrix} + r \begin{bmatrix} -\sin(\theta)\frac{\partial \theta}{\partial p_1} & -\sin(\theta)\frac{\partial \theta}{\partial p_2} \\ \cos(\theta)\frac{\partial \theta}{\partial p_1} & \cos(\theta)\frac{\partial \theta}{\partial p_2} \end{bmatrix} \\ &= \begin{bmatrix} \cos(\theta) \\ \sin(\theta) \end{bmatrix} \begin{bmatrix} \frac{\partial r}{\partial p_1} & \frac{\partial r}{\partial p_2} \end{bmatrix} + r \begin{bmatrix} -\sin(\theta) \\ \cos(\theta) \end{bmatrix} \begin{bmatrix} \frac{\partial \theta}{\partial p_1} & \frac{\partial \theta}{\partial p_2} \end{bmatrix} \\ &= \begin{bmatrix} \cos(\theta) \\ \sin(\theta) \end{bmatrix} \frac{\partial r}{\partial p} + r \begin{bmatrix} -\sin(\theta) \\ \cos(\theta) \end{bmatrix} \frac{\partial \theta}{\partial p}. \end{aligned}$$

With the definition $J = \left[\begin{smallmatrix} 0 & -1 \\ 1 & 0 \end{smallmatrix}\right]$ and the observations that

$$\frac{p}{r} = \begin{bmatrix} \cos(\theta) \\ \sin(\theta) \end{bmatrix} \quad \text{and} \quad Jp = r \begin{bmatrix} -\sin(\theta) \\ \cos(\theta) \end{bmatrix}, \tag{8}$$

for $r \neq 0$, the calculations above can be further simplified and summarized as

$$I = \frac{\partial p}{\partial p} = \frac{\partial}{\partial p}\left(r \begin{bmatrix} \cos(\theta) \\ \sin(\theta) \end{bmatrix} \right) = \frac{1}{r} p \frac{\partial r}{\partial p} + Jp \frac{\partial \theta}{\partial p}. \tag{9}$$

Note that $p^T J p = 0$ follows from the definition of J. Hence, left-multiplying (9) by p^T gives

$$p^T = \tfrac{1}{r} p^T p \tfrac{\partial r}{\partial p} + p^T J p \tfrac{\partial \theta}{\partial p} = \tfrac{r^2}{r}\tfrac{\partial r}{\partial p} = r\tfrac{\partial r}{\partial p}.$$

Similarly, the following equations hold

$$(Jp)^T I = \tfrac{1}{r} p^T J^T p \tfrac{\partial r}{\partial p} + p^T p \tfrac{\partial \theta}{\partial p} = r^2 \tfrac{\partial \theta}{\partial p},$$

which leads to the partial derivatives

$$\tfrac{\partial r}{\partial p} = \tfrac{1}{r} p^T \quad \text{and} \quad \tfrac{\partial \theta}{\partial p} = \tfrac{1}{r^2}(Jp)^T. \tag{10}$$

With these calculations, the definition of the function f_B follows from (1):

$$\begin{aligned} \dot{r} &= \tfrac{\partial r}{\partial p}\dot{p} = \tfrac{1}{r} p^T \dot{p} = \tfrac{1}{r}\left[r\cos(\theta) \ \ r\sin(\theta) \right] \left[\begin{smallmatrix} u_1\cos(\phi) \\ u_2\sin(\phi) \end{smallmatrix}\right] \\ &= u_1[\cos(\theta)\cos(\phi) - \sin(\theta)\sin(\phi)] = v_1 r\cos(\phi - \theta) \\ &= v_1 r\cos(-\beta_\mathrm{R} - \alpha_\mathrm{R} + \beta_\mathrm{R}) = v_1 r\cos(\alpha_\mathrm{R}) \\ \dot{\theta} &= \tfrac{\partial \theta}{\partial p}\dot{p} = \tfrac{1}{r^2} p^T J^T \dot{p} = \tfrac{1}{r^2}\left[r\cos(\theta) \ \ r\sin(\theta) \right] \left[\begin{smallmatrix} u_1\sin(\phi) \\ -u_1\cos(\phi) \end{smallmatrix}\right] \\ &= u_1(\cos(\theta)\sin(\phi) - \sin(\theta)\cos(\phi)) = v_1\sin(\phi - \theta)\alpha_\mathrm{R}) \\ &= -v_1\sin(\alpha_\mathrm{R}) \\ \dot{\beta}_\mathrm{R} &= -\dot{\phi} = -v_2 \\ \dot{\alpha}_\mathrm{R} &= \dot{\beta}_\mathrm{R} + \dot{\theta} = -v_2 - v_1\sin(\alpha_\mathrm{R}). \end{aligned}$$

Observe that for f_F we need to consider the relation $\alpha_\mathrm{R} = \alpha_\mathrm{F} - \pi$ and thus the representation f_F follows. □

While Lemma 1 excludes the case $r = 0$, note that the functions f_R and f_F are well-defined for $r = 0$.

3. LOCAL CONTROLLER DESIGN

In this section, we derive control laws locally asymptotically stabilizing the set

$$\mathcal{A} = \{0\} \times \mathbb{R} \times \{0\} \tag{11}$$

as well as the origin of the dynamical system (6). The Lyapunov construction is inspired by Aicardi et al. (1995).

Lemma 2. Let the feedback gains $k_r, k_\alpha \in \mathbb{R}_{>0}$ be arbitrary. Consider the dynamics (6) with $z_\mathrm{R} \in \mathcal{Z}$. Then

$$v_\mathrm{R} = \begin{bmatrix} -k_r\cos(\alpha_\mathrm{R}) \\ k_r\cos(\alpha_\mathrm{R})\sin(\alpha_\mathrm{R}) + k_\alpha\alpha_\mathrm{R} \end{bmatrix} \tag{12}$$

locally asymptotically stabilizes the set $\mathcal{A}$ in (11). Moreover, $V(z_\mathrm{R}) = \frac{1}{2}(r^2 + \alpha_\mathrm{R}^2)$ is a Lyapunov function for the closed-loop dynamics with respect to $\mathcal{A}$. ⌟

Proof. First observe that $\frac{1}{2}|z_\mathrm{R}|_\mathcal{A}^2 \leq V(z_\mathrm{R}) \leq \frac{1}{2}|z_\mathrm{R}|_\mathcal{A}^2$, i.e., V radially unbounded. Moreover, the directional derivative of V along the dynamics satisfies

$$\begin{aligned}\langle \nabla V(z_{\mathrm{R}}), f_{\mathrm{R}}(z_{\mathrm{R}}, v_{\mathrm{R}})\rangle &= r^2 v_{\mathrm{R}_1}\cos(\alpha_{\mathrm{R}}) + \alpha(-v_{\mathrm{R}_2} - v_{\mathrm{R}_1}\sin(\alpha_{\mathrm{R}})) \\ &= -k_r r^2\cos^2(\alpha_{\mathrm{R}}) - k_\alpha \alpha_{\mathrm{R}}^2 < 0,\end{aligned}$$

and thus $\frac{d}{dt}V(z_{\mathrm{R}}(t)) < 0$ for all $z_{\mathrm{R}} \in \mathbb{R}^3 \backslash \mathcal{A}$ which implies asymptotic stability of $\mathcal{A}$. □

To additionally ensure that $\beta_{\mathrm{R}}(t) \to 0$ for $t \to \infty$, we may include an additional term in the feedback law v_{R} and in the Lyapunov function.

Lemma 3. Let $k_r, k_\alpha, k_\beta \in \mathbb{R}_{>0}$ be arbitrary. Consider the dynamics (6) with $z_{\mathrm{R}} \in \mathcal{Z}$. Then the control law

$$v_{\mathrm{R}} = \begin{bmatrix} -k_r\cos(\alpha_{\mathrm{R}}) \\ k_r\cos(\alpha_{\mathrm{R}})\sin(\alpha_{\mathrm{R}}) + k_\alpha\alpha_{\mathrm{R}} + k_\beta(\alpha_{\mathrm{R}} - \beta_{\mathrm{R}})\frac{\cos(\alpha_{\mathrm{R}})\sin(\alpha_{\mathrm{R}})}{\alpha_{\mathrm{R}}} \end{bmatrix} \tag{13}$$

is well-defined for all $z_{\mathrm{R}} \in \mathcal{Z}$, locally asymptotically stabilizes the origin $0 \in \mathbb{R}^3$ and $V(z_{\mathrm{R}}) = \frac{1}{2}(r^2 + \frac{k_\beta}{k_r}(\alpha_{\mathrm{R}} - \beta_{\mathrm{R}})^2 + \alpha_{\mathrm{R}}^2)$ is monotonically decreasing for all $z_{\mathrm{R}} \in \mathcal{Z}$. ⌟

Proof. First note that $\lim_{\alpha_{\mathrm{R}}\to 0}\frac{\sin(\alpha_{\mathrm{R}})}{\alpha_{\mathrm{R}}} = 1$ and thus the feedback law is well-defined. Moreover, since the matrix $\begin{bmatrix} k_\beta + k_r & -k_\beta \\ -k_\beta & k_\beta \end{bmatrix}$ is positive definite, V is radially unbounded. Extending the derivations in Lemma 2, it holds that

$$\begin{aligned}&\langle \nabla V(z_{\mathrm{R}}), f_{\mathrm{R}}(z_{\mathrm{R}}, v_{\mathrm{R}})\rangle \\ &= r^2 v_{\mathrm{R}_1}\cos(\alpha_{\mathrm{R}}) + \tfrac{k_\beta}{k_r}(-v_{\mathrm{R}_2} - v_{\mathrm{R}_1}\sin(\alpha_{\mathrm{R}}) + v_{\mathrm{R}_2})(\alpha_{\mathrm{R}} - \beta_{\mathrm{R}}) \\ &\quad + \alpha_{\mathrm{R}}(-v_{\mathrm{R}_2} - v_{\mathrm{R}_1}\sin(\alpha_{\mathrm{R}})) \\ &= -k_r r^2\cos^2(\alpha_{\mathrm{R}}) - k_\alpha\alpha_{\mathrm{R}}^2 + k_\beta(\alpha_{\mathrm{R}} - \beta_{\mathrm{R}})\cos(\alpha_{\mathrm{R}})\sin(\alpha_{\mathrm{R}}) \\ &\quad - \alpha_{\mathrm{R}} k_\beta(\alpha_{\mathrm{R}} - \beta_{\mathrm{R}})\left(\cos(\alpha_{\mathrm{R}})\tfrac{\sin(\alpha_{\mathrm{R}})}{\alpha_{\mathrm{R}}}\right) \\ &= -k_r r^2\cos^2(\alpha_{\mathrm{R}}) - k_\alpha\alpha_{\mathrm{R}}^2 \le 0 \quad \forall\, z_{\mathrm{R}} \in \mathcal{Z}\end{aligned}$$

and thus, local stability of the origin follows. Moreover, for all $z_{\mathrm{R}} \in \mathcal{Z}$ for which V is not strictly decreasing it holds that $\dot{z}_{\mathrm{R}}^T = [\,0\ k_\beta\beta_{\mathrm{R}}\ k_\beta\beta_{\mathrm{R}}\,]$, whose right-hand side is unequal to zero for all $\beta_{\mathrm{R}} \neq 0$. Hence, local asymptotic stability follows from the Krasovskii-LaSalle invariance theorem (Vidyasagar, 1993, Theorem 5.3.77). □

Observe that through $k_\beta = 0$, Lemma 3 covers the result of Lemma 2 as a special case because (13) reduces to (12). For the z_{F}-dynamics in (6), using the same ideas, a result equivalent to Lemma 3 can be derived. We summarize this result in the following corollary.

Corollary 1. Let $k_r, k_\alpha, k_\beta \in \mathbb{R}_{>0}$ be arbitrary. Consider the dynamics (6) with $z_{\mathrm{F}} \in \mathcal{Z}$. Then the control law

$$v_{\mathrm{F}} = \begin{bmatrix} k_r\cos(\alpha_{\mathrm{F}}) \\ k_r\cos(\alpha_{\mathrm{F}})\sin(\alpha_{\mathrm{F}}) + k_\alpha\alpha_{\mathrm{F}} + k_\beta(\alpha_{\mathrm{F}} - \beta_{\mathrm{F}})\frac{\cos(\alpha_{\mathrm{F}})\sin(\alpha_{\mathrm{F}})}{\alpha_{\mathrm{F}}} \end{bmatrix} \tag{14}$$

is well-defined for all $z_{\mathrm{F}} \in \mathcal{Z}$, locally asymptotically stabilizes the origin $0 \in \mathbb{R}^3$ and $V(z_{\mathrm{F}}) = \frac{1}{2}(r^2 + \frac{k_\beta}{k_r}(\alpha_{\mathrm{F}} - \beta_{\mathrm{F}})^2 + \alpha_{\mathrm{F}}^2)$ is monotonically decreasing for all $z_{\mathrm{F}} \in \mathcal{Z}$. ⌟

4. A GLOBAL HYBRID STABILIZER

In this section we combine the two local control laws introduced in the preceding section in a hybrid systems formulation. As a first step, we introduce an additional discrete variable $q \in \{-1, 1\}$ where $q = -1$ represents the rear camera R and $q = 1$ represents the front camera F. In the overall system representation we consider the state

$$\xi = [r\ \beta\ \alpha\ q]^T \in \Xi \tag{15a}$$

where the pair (α, β) can either represent $(\alpha_{\mathrm{R}}, \beta_{\mathrm{R}})$ when $q = -1$ or $(\alpha_{\mathrm{F}}, \beta_{\mathrm{F}})$ when $q = 1$ and where the domain Ξ is defined as

$$\Xi := \mathbb{R}_{\ge 0} \times \mathbb{R} \times [-\tfrac{\pi}{2} - \delta, \tfrac{\pi}{2} + \delta] \times \{-1, 1\} \tag{15b}$$

for $\delta \in (0, \frac{\pi}{2})$. With this definition, the dynamics (6) can be summarized through the flow map

$$\dot{\xi} = \begin{bmatrix} \dot{r} \\ \dot{\beta} \\ \dot{\alpha} \\ \dot{q} \end{bmatrix} = \begin{bmatrix} -q v_1 r\cos(\alpha) \\ -v_2 \\ -v_2 + q v_1\sin(\alpha) \\ 0 \end{bmatrix}, \quad \xi \in \mathcal{C} \tag{15c}$$

and the feedback laws (13) and (14) are captured through

$$v = \begin{bmatrix} q k_r\cos(\alpha) \\ k_r\cos(\alpha)\sin(\alpha) + k_\alpha\alpha + k_\beta(\alpha - \beta)\cos(\alpha)\frac{\sin(\alpha)}{\alpha} \end{bmatrix} \tag{15d}$$

The set $\mathcal{C}$, denoting the flow set, is defined as

$$\mathcal{C} := \{\xi \in \Xi : |\alpha| \le \tfrac{\pi}{2} + \delta, |\beta| \le \tfrac{3}{2}\pi + \delta\}.$$

For the jump map and the jump set, we first define the functions

$$g_\beta(\xi) = \begin{bmatrix} r \\ \beta - 2\pi\,\mathrm{sign}(\beta) \\ \alpha \\ q \end{bmatrix}, \quad g_\alpha(\xi) = \begin{bmatrix} r \\ \beta \\ \alpha - \pi\,\mathrm{sign}(\alpha) \\ -q \end{bmatrix}$$

and the sets

$$\begin{aligned}\mathcal{D}_\alpha &:= \{\xi \in \Xi : |\alpha| \ge \tfrac{\pi}{2} + \delta \ \wedge\ |\beta| \le \tfrac{3}{2}\pi + \delta\}, \\ \mathcal{D}_\beta &:= \{\xi \in \Xi : |\beta| \ge \tfrac{3}{2}\pi + \delta\}.\end{aligned}$$

Then the jump map is defined as

$$\xi^+ \in G(\xi) = \begin{cases} \{g_\beta(\xi)\} & \text{if } \xi \in \mathcal{D}_\beta \backslash \mathcal{D}_\alpha, \\ \{g_\alpha(\xi)\} & \text{if } \xi \in \mathcal{D}_\alpha \backslash \mathcal{D}_\beta, \\ \{g_\alpha(\xi)\} \cup \{g_\beta(\xi)\} & \text{if } \xi \in \mathcal{D}_\alpha \cap \mathcal{D}_\beta, \end{cases} \tag{15e}$$

and the jump set is defined as the union

$$\mathcal{D} := \mathcal{D}_\beta \cup \mathcal{D}_\alpha. \tag{15f}$$

Note that $\beta^+ = \beta - 2\pi\,\mathrm{sign}(\beta)$ defined through g_β guarantees that β^+ and β differ by a multiple of 2π and $|\beta^+| < |\beta|$ for all $\xi \in \mathcal{D}_\beta$ (wherein $|\beta| \ge \frac{3}{2}\pi + \delta$). Thus, β^+ and β describe the same information with respect to the position of the robot but β^+ is closer to the target orientation $\beta = 0$. Similarly, $\alpha^+ = \alpha - \pi\,\mathrm{sign}(\alpha)$ defined through g_α captures the properties in (5) when the perspective of the cameras is switched. Additionally, from the definition of the hybrid system it is clear that multiple consecutive jumps are possible, but, due to the selection of the parameter δ, Zeno behavior is not possible. Finally, since (15) satisfies (Goebel et al., 2012, As. 6.5), then asymptotic stability is robust in the sense of (Goebel et al., 2012, Ch. 7).

Theorem 1. Let $\delta \in (0, \frac{\pi}{2})$, $k_r, k_\alpha \in \mathbb{R}_{>0}$ and $k_\beta \in (0, \frac{2\delta k_r}{3\pi}]$ be arbitrary. Then, the set $\mathcal{A}_q = \{0\} \times \{0\} \times \{0\} \times \{-1, 1\}$ is globally robustly asymptotically stable for the hybrid closed-loop system dynamics (15). Moreover, $V(\xi) = \frac{1}{2}(r^2 + \frac{k_\beta}{k_r}(\alpha - \beta)^2 + \alpha^2)$ is monotonically decreasing along solutions $\xi : \mathrm{dom}(\xi) \to \Xi$. ⌟

Proof. We have established local properties of the closed-loop dynamics in Lemma 3 and in Corollary 1. What is left to show, is that the function V is decreasing at discrete time updates. Let $\xi \in \mathcal{D}_\beta$. Then it holds that

$$\begin{aligned}V(\xi^+) - V(\xi) &= \tfrac{k_\beta}{2k_r}(\alpha^+ - \beta^+)^2 - \tfrac{k_\beta}{2k_r}(\alpha - \beta)^2 \\ &= \tfrac{k_\beta}{2k_r}\left[4(\alpha - \beta)\,\mathrm{sign}(\beta)\pi + 4\pi^2\right] \\ &= 2\tfrac{k_\beta}{k_r}\left[\alpha\,\mathrm{sign}(\beta)\pi - \beta\,\mathrm{sign}(\beta)\pi + \pi^2\right]\end{aligned}$$

$$\leq 2\frac{k_\beta}{k_r}\left[(\tfrac{\pi}{2}+\delta)\pi - (\tfrac{3}{2}\pi+\delta)\pi + \pi^2\right] = 0.$$

Similarly, for $\xi \in \mathcal{D}_\alpha$ it holds that

$$\begin{aligned}
V(\xi^+) - V(\xi) &= \tfrac{k_\beta}{2k_r}(\alpha^+ - \beta^+)^2 + \tfrac{1}{2}(\alpha^+)^2 - \tfrac{k_\beta}{2k_r}(\alpha-\beta)^2 - \tfrac{1}{2}\alpha^2 \\
&= \tfrac{k_\beta}{k_r}(\alpha-\beta)\,\mathrm{sign}(\alpha)\pi + \tfrac{k_\beta}{2k_r}\pi^2 - |\alpha|\pi + \tfrac{1}{2}\pi^2 \\
&= -\tfrac{k_\beta}{k_r}|\alpha|\pi + \tfrac{k_\beta}{k_r}\beta\,\mathrm{sign}(\alpha)\pi + \tfrac{k_\beta}{2k_r}\pi^2 - |\alpha|\pi + \tfrac{1}{2}\pi^2 \\
&= -\tfrac{k_\beta}{k_r}|\alpha|\pi + \beta\,\mathrm{sign}(\alpha)\pi + \tfrac{k_\beta}{2k_r}\pi^2 - |\alpha|\pi + \tfrac{1}{2}\pi^2 \\
&\leq -\tfrac{k_\beta}{k_r}(\tfrac{\pi}{2}+\delta)\pi + \tfrac{k_\beta}{k_r}(\tfrac{3\pi}{2}+\delta)\pi + \tfrac{k_\beta}{2k_r}\pi^2 - (\tfrac{\pi}{2}+\delta)\pi + \tfrac{1}{2}\pi^2 \\
&\leq -\delta\pi + \tfrac{3}{2}\tfrac{k_\beta}{k_r}\pi^2 \leq 0
\end{aligned}$$

and where the last inequality follows from the assumption $k_\beta \leq \frac{2\delta k_r}{3\pi}$. Thus, V is monotonically decreasing and we can conclude global asymptotic stability. Finally, robustness follows from (Goebel et al., 2012, Thm 7.21). □

5. NUMERICAL SIMULATIONS

We illustrate the results derived in the preceding section based on numerical simulations. Figure 3 shows closed-loop solutions using the feedback law (15d) with $k_\beta = 0$, i.e., the final orientation ϕ (or β) is not penalized. In particular, closed-loop solutions for various initial conditions in the (p_1, p_2)-plane, as well as the evolution over time in the x and z coordinates are shown. The remaining gains are defined as $k_r = 2$ and $k_\alpha = 1$, respectively. Additionally, the parameter $\delta = \frac{\pi}{10}$ is used for the simulations. To illustrate robustness properties of the controller, ξ is replaced by $\xi + [\varepsilon_r\ \varepsilon_\beta\ \varepsilon_\alpha\ 0]^T$ in the right-hand side of (15c) in the simulations, where ε_r, ε_β and ε_α represent white Gaussian noise with zero mean and standard deviations $\sigma_r = 0.05$, $\sigma_\beta = \sigma_\alpha = \frac{3\pi}{180}$. As expected from the theoretical results, r and α converge to to origin, while the angle β does not necessarily converge to zero.

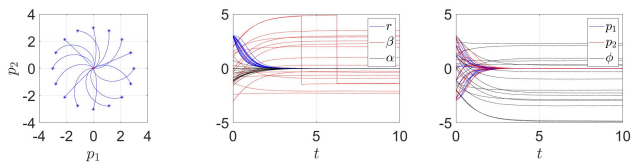

Fig. 3. Closed-loop solutions of the hybrid system (15) with controller gain $k_\beta = 0$.

For the simulations in Figure 4 the gain $k_\beta = 0$ has been replaced by $k_\beta = \frac{2\delta k_r}{3\pi}$. As expected, the controller ensures that additionally the orientation in terms of β or ϕ, respectively converges to zero for $t \to \infty$ according to Theorem 1. Figure 4 additionally shows the decrease of the function V defined in Theorem 1.

6. CONCLUSIONS

Inspired by the controller design in Aicardi et al. (1995), in this work we have proposed a globally stabilizing controller for unicycle dynamics relying on a hybrid systems formulation. The controller is motivated through mobile robots equipped with range sensors and front and rear cameras with overlapping fields of view.

While the control law derived in Theorem 1 is unbounded, a bounded globally stabilizing control law can be obtained by appropriately scaling v in (15d) (see (Braun et al., 2021, Theorem 2.3), for example). Such a scaling can also be used to handle unknown input gains, which have been encountered for example in Vinco et al. (2021), where the input gain depends on the (unknown) state of charge of the battery. Future work will focus on the analysis of robustness properties of the controller and will incorporate obstacle avoidance properties in the overall controller design. In this context we will take inspiration from Braun and Zaccarian (2021) and Marley et al. (2021).

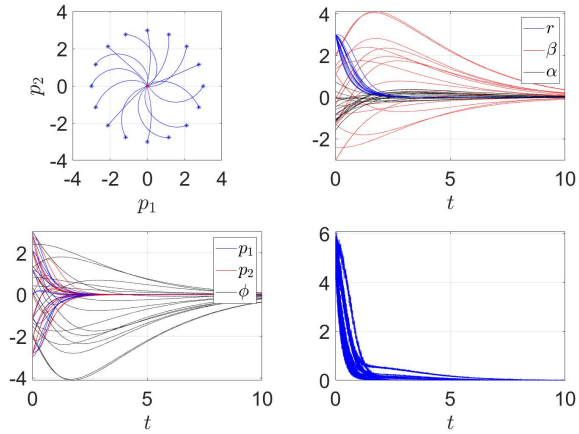

Fig. 4. Closed loop solutions of the hybrid system (15).

REFERENCES

Aicardi, M., Casalino, G., Bicchi, A., and Balestrino, A. (1995). Closed loop steering of unicycle like vehicles via lyapunov techniques. *IEEE Robotics Automation Magazine*, 2(1), 27–35.

Braun, P., Grüne, L., and Kellett, C.M. (2021). *(In-)Stability of Differential Inclusions: Notions, Equivalences, and Lyapunov-like Characterizations*. Springer.

Braun, P. and Zaccarian, L. (2021). Augmented obstacle avoidance controller design for mobile robots. *IFAC-PapersOnLine*, 54(5), 157–162. 7th IFAC Conference on Analysis and Design of Hybrid Systems.

Brockett, R.W. (1983). Asymptotic stability and feedback stabilization. *Differential Geometric Control Theory*, 27(1), 181–191.

Goebel, R., Sanfelice, R.G., and Teel, A.R. (2012). *Hybrid Dynamical Systems: Modeling, Stability, and Robustness*. Princeton University Press.

Marley, M., Skjetne, R., and Teel, A.R. (2021). Synergistic control barrier functions with application to obstacle avoidance for nonholonomic vehicles. In *2021 American Control Conference*, 243–249.

Nešić, D., Teel, A., and Zaccarian, L. (2011). Stability and performance of SISO control systems with First Order Reset Elements. *IEEE Trans. on Automatic Control*, 56(11), 2567–2582.

Sontag, E.D. (1999). Nonlinear feedback stabilization revisited. In *Dynamical Systems, Control, Coding, Computer Vision*, 223–262. Birkhäuser Basel.

Tzafestas, S.G. (2013). *Introduction to Mobile Robot Control*. Elsevier.

Vidyasagar, M. (1993). *Nonlinear Systems Analysis: Second Edition*. Prentice-Hall.

Vinco, G.M., Braun, P., and Zaccarian, L. (2021). A modular architecture for mobile robots equipped with continuous-discrete observers. In *IEEE International Conference on Mechatronics*, 1–6.